Interfacial self-assembly of a bacterial hydrophobin

Interfacial self-assembly of a bacterial hydrophobin

Keith M. Bromley[a], Ryan J. Morris[a], Laura Hobley[b], Giovanni B. Brandani[a], Matthew McCluskey[a], Ulrich Zachariae[c], Davide Marenduzzo[a], Nicola R. Stanley-Wall[b], and Cait. E. MacPhee[a]

[a]James Clerk Maxwell Building, School of Physics, University of Edinburgh, Edinburgh EH9 3JZ, United Kingdom

[b]Division of Molecular Microbiology, College of Life Sciences, University of Dundee, Dundee DD1 5EH, United Kingdom

[c]Division of Computational Biology, College of Life Sciences, University of Dundee, Dundee DD1 5EH, United Kingdom

Corresponding author: Prof. Cait MacPhee

James Clerk Maxwell Building, School of Physics, University of Edinburgh, Edinburgh EH9 3JZ, United Kingdom

Email: cait.macphee@ed.ac.uk

Running Title: Bacterial hydrophobin self-assembly

Classification: Biological Sciences: Biophysics and Computational Biology

Keywords: *Bacillus subtilis*, biofilm, BslA, hydrophobin, interfacial self-assembly

Abstract

The majority of bacteria live within the confines of a biofilm in the natural environment. The Gram-positive bacterium *Bacillus subtilis* forms biofilms that exhibit a characteristic wrinkled morphology and a highly hydrophobic surface. A critical component in generating these properties is the protein BslA, which forms a coat across the surface of the sessile community. We recently reported the structure of BslA and noted its similarity to a class of surface-active proteins known as hydrophobins, thereby designating BslA as the first structurally defined "bacterial hydrophobin". Here, we describe the mechanism by which BslA stabilises air- and oil-water interfaces. Specifically, we found that the amino acids making up a large, surface-exposed hydrophobic cap in the crystal structure are shielded in aqueous solution by adopting a random coil conformation. At an interface, these cap residues refold to form a β-sheet, inserting the hydrophobic side chains into the air or oil phase. The requirement for this refolding event results in an energetic barrier to adsorption by wild-type (WT)-BslA. By replacing a hydrophobic leucine in the centre of the cap with a positively charged lysine, we eliminated the barrier to adsorption, indicating that the mutation disrupts the shielding mechanism in the cap. Additionally, while WT-BslA organises into a 2D rectangular lattice after adsorption, self-assembly by L77K-BslA is impaired. The lateral interactions that facilitate the organisation of WT-BslA are likely responsible for enhanced stability of WT-BslA films compared to BslA-L77K films. This limited structural metamorphosis represents a previously unidentified mechanism to interfacial stabilisation by proteins.

Significance Statement

In the natural environment the majority of bacteria live within the confines of a structured social community called a biofilm. The stability of biofilms arises from the extracellular matrix, which consists of proteins, polysaccharides and extracellular DNA. One of these proteins, BslA, forms a hydrophobic "raincoat" at the surface of the biofilm. We have uncovered the mechanism that enables this protein to function, revealing a structural metamorphosis from a form that is stable in water, to a structure that prefers the interface, where it self-assembles with nanometre precision to form a robust film. Our findings have wide-ranging implications, from the disruption of harmful bacterial biofilms, to the generation of nanoscale materials.

Introduction

In the natural environment the majority of bacteria live within the confines of a structured social community called a biofilm. Residence offers bacteria multiple advantages over their free-living cousins that cannot be explained by genetics (1). Many of these benefits are conferred by production of an extracellular matrix, the hallmark feature of biofilms. The biofilm matrix largely consists of proteins, polysaccharides and DNA. It provides a source of water and nutrients, and confers structural integrity (1–4). Biofilms formed by the Gram-positive bacterium *Bacillus subtilis* are characterised by a highly wrinkled morphology and a hydrophobic surface. The biofilm matrix is composed of a large exopolysaccharide synthesized by the products of the *epsA-O* operon, and the TasA/TapA proteins that form amyloid-like fibres. Assembly of the matrix requires the small, secreted surface-active protein called BslA (formerly YuaB). BslA is found as a discrete layer at the surface of the biofilm despite uniform transcription of the coding region by the entire biofilm population (5–8). It achieves its surface hydrophobicity due to its striking amphiphilic structure, which we recently elucidated by X-ray crystallography (9). The structure of BslA consists of a canonical immunoglobulin-like domain, to which is appended a three-stranded 'cap' that is highly hydrophobic in character, containing leucine residues as well as isoleucine, valine and alanine (9). In the crystal structure, this cap comprises a surface-exposed hydrophobic patch of ~1620 Å that we have previously proposed to mediate adsorption to the air/water interface.

We previously demonstrated the importance of the hydrophobic cap in controlling the functional properties of BslA by studying the effect of replacing hydrophobic leucine residues in the cap region with positively charged lysine residues (mutants L76K, L77K and L79K) (9). *In vivo*, the mutations caused the biofilms to form without a wrinkled morphology and two of the mutations (L77K and L79K) drastically reduced the hydrophobicity of the biofilm surface, as measured by a reduction in contact angle. *In vitro*, all three mutant proteins successfully formed a film at an oil-water interface in a pendant drop tensiometer, and this film was viscoelastic as indicated by the formation of wrinkles

following compression of the droplet. However, the mutant and wild-type (WT) proteins behaved differently after compression of the film: while the wrinkles formed in the WT-BslA film did not relax over the period of the experiment (10 minutes), the wrinkles formed in films assembled from mutant proteins fully relaxed, suggesting ejection of mutant protein from the interface and indicating that the hydrophobic cap plays an important role in the stability of BslA films.

The large surface-exposed hydrophobic patch exhibited by BslA is a characteristic shared by the unrelated family of fungal proteins known as the hydrophobins (10). Hydrophobins are a conserved family of surface-active proteins that, among other functions, lower the surface tension of growth medium, allowing fungal hyphae to penetrate the air-water interface. The hydrophobins are divided into class I and class II; class I proteins form robust amyloid-like rodlets at the air-water interface, whereas class II proteins reduce surface tension by forming ordered lattices of native-like protein at the interface. In both classes, eight canonical cysteine residues form a highly conserved series of disulphide bridges that provide a rigid framework that restricts the mobility of the polypeptide chain (11, 12). In the class II hydrophobins this framework is thought to stabilise the surface exposure of the large hydrophobic patch that mediates interfacial assembly (13). It is the formation of a large hydrophobic patch, rather than any sequence similarity, that caused us to classify BslA as a bacterial hydrophobin. An outstanding question remains, however: in the absence of a stabilising disulphide-bonded network, how is the large surface-exposed hydrophobic patch of BslA stabilised sufficiently in aqueous environments to mediate the surface-activity of the protein?

Here we use WT-BslA and the L77K mutant to determine the mechanism that enables BslA to partition from the aqueous phase to the interface, where it decreases the interfacial tension and self-assembles to form a stable viscoelastic film. We show that although WT-BslA binds strongly to interfaces, it needs to overcome a barrier to adsorption, whereas the L77K mutant binds to an interface in a diffusion-limited manner. Once WT-BslA has bound to the interface, it undergoes a conformational change to a structure enriched in β-sheet, and the proteins become organised into a 2D rectangular lattice. Through examination of the decameric crystal structure in conjunction with circular dichroism spectroscopy, our data indicate that the cap region is disordered in aqueous solution, with many of the hydrophobic amino acids buried. On binding to the interface, we propose that the hydrophobic amino acids in the cap become fully exposed to the hydrophobic environment and adopt an extended conformation that may participate in long-range intermolecular β-sheet interactions. The hydrophobic cap is essential for this function, since although the L77K mutant also exhibits increased β-sheet content at an interface, we observe a loss of long-range intermolecular order that leads to the decreased stability of the BslA-L77K film. Together these data present a previously uncovered structural metamorphosis that enables interfacial stabilisation by proteins.

Results

One possible mechanism for stabilisation of the large hydrophobic cap region in BslA is the formation of higher order oligomers, such as the decamer observed in the crystal structure. Indeed, formation of a tetramer has been observed for the class II fungal hydrophobin HFB II (14). Although size exclusion chromatography indicated that purified BslA forms a mixture of monomers, dimers and higher order oligomers (Figure S1), addition of a reducing agent such as DTT or BME yields a sample containing purely monomeric protein (Figure S2 and S3). BslA contains two closely-spaced cysteine residues, and it is as yet unclear whether these residues play a role in biofilm formation or maturation. We established that the monomeric protein is stable and soluble over a timescale of days, suggesting that the large hydrophobic cap we observed in the crystal structure is shielded in aqueous solution, likely through some form of structural rearrangement. All experiments presented here used monomeric protein (unless stated), as purified dimeric protein gave equivalent results if it is assumed that the concentration of surface-active species comprises 50% of the protein concentration of the sample (i.e. only one subunit of the disulphide-bonded dimer is available for surface activity; Figure S4).

WT-BslA reduces the surface tension of water. BslA functions in vivo to aid in the erection of aerial structures in the biofilm (9, 15), a role that is suggestive of the capability to reduce the surface tension of water. Pendant drop tensiometry was performed on aqueous droplets of BslA to observe the change in interfacial tension over time. In this technique, the shape of a drop is fitted to the Young-Laplace equation to measure the interfacial tension (IFT) at the droplet surface (16, 17), which usually decreases as the interface is populated by surface active species (18). An

increase in the error of the fit to the Young-Laplace equation indicates that a viscoelastic film has formed at the interface, and since a solid layer now separates the two liquid phases the concept of interfacial tension no longer applies (19). Figure 1a shows the change in IFT of droplets of unfractionated WT-BslA suspended in air and in oil. Typically, the interfacial tension of the water-air or water-oil interface drops after a lag period during which the population of protein at the interface is increasing. The magnitude of the decrease in IFT caused by BslA was consistently smaller than the typical drop in IFT observed for the class II fungal hydrophobin HFBII at similar concentrations and time scales (19). For example, at 0.02 $mg.mL^{-1}$ and 300 s, BslA decreases the apparent IFT to 70.8 ± 1 $mN.m^{-1}$, whereas HFBII decreases the IFT to ~56 $mN.m^{-1}$ under the same conditions (19). However, despite this comparatively small decrease in IFT, the increase in the error of the Laplace fit (Figure S6) indicates that a BslA film has already formed by 300 s, whereas HFBII must lower the IFT to at least 50 $mN.m^{-1}$ before the error of the Laplace fit increases (19).

Previously, the viscoelastic film formed by the class II fungal hydrophobin HFBI was shown to cause a sessile drop to develop a planar surface after 30 minutes on a hydrophobic material (20), indicating that the protein film formed at the interface has a sufficiently high elastic modulus as to deform the droplet shape (21). In contrast, WT-BslA does not deform sessile drops at 0.01, 0.03 and 0.1 $mg.mL^{-1}$ after thirty minutes, even though visual inspection confirmed the formation of a viscoelastic film in each case (Figure 1b). The formation of such a film was additionally confirmed at water-air or water-oil interfaces by the appearance of persistent wrinkles on the surface of pendant drops following compression (9). Figure 1c shows a WT-BslA droplet suspended in air before and after compression, while the WT-BslA droplet depicted in Figure 1d was suspended in triglyceride oil. Taken together our results indicate that BslA forms interfacial films at lower protein densities than the class II fungal hydrophobins, and that the resulting films, while very stable, can form without causing a significant deformation in droplet shape.

WT-BslA has a barrier to adsorption to an air-water interface, whereas BslA-L77K does not. Pendant drop tensiometry with drop shape analysis was performed on BslA solutions at concentrations between 0.01 and 0.1 $mg.mL^{-1}$. At low protein concentrations, the IFT initially remains unchanged for a lag time that is designated "Regime I" (22, 23) (Figure 1a). During this period the interface becomes occupied by protein to a critical surface coverage above 50% (22), and provides a measure of the rate at which the protein partitions to the interface. During Regime II, the IFT decreases steeply until the interface is saturated with adsorbed protein. Following saturation, the IFT levels off (Regime III), although a shallow gradient often indicates rearrangement of the protein layer. Although these characteristics can be seen in typical BslA dynamic interfacial tension response curves, the fit error of the Young Laplace equation to the droplet increased at some point during most experiments, indicating the formation of a viscoelastic layer (19).

The time (t) it takes for a particle to adsorb onto an interface via diffusion can be predicted by Equation 1 (24):

$$\Gamma(t) = 2C_b\sqrt{\frac{Dt}{\pi}} \qquad (1)$$

where Γ is surface concentration, C_b is bulk concentration and D is the diffusion coefficient of the particle. Equation 1 assumes that C_b is unchanging and that there is no back diffusion from the interface (24). We can estimate Γ_{max} (for 100% surface coverage) to be 1.57 $mg.m^{-2}$ from TEM images of the BslA 2D lattice (Figure 4a), while D was measured to be 9.87×10^{-7} $cm^2.s^{-1}$ for monomeric BslA using dynamic light scattering (DLS; Figure S5). In cases where the error of the Laplace fit increased before a decrease in IFT was observed, then the onset time of any increase in the error of the Laplace fit was used (Figure S6).

Figure 2 shows a plot of Regime I time against BslA concentration for WT-BslA and BslA-L77K as well as the "ideal" Regime I times calculated from Equation 1 (dashed line). The results clearly demonstrate that WT-BslA takes more time to decrease the interfacial tension of a droplet (or increase the error of Laplace fit) in air than would be expected for a system that did not exhibit an adsorption barrier or back diffusion. In contrast, the BslA-L77K mutant reduced the interfacial tension of the droplet within the maximum calculated time for particles of equivalent size with no adsorption barrier. Under diffusion-limiting conditions, as determined by Equation 1, BslA at a concentration of

0.03 mg.mL^{-1} should take 22 s to reach a surface concentration of 1.57 mg.m^{-2}. As the IFT will begin to decrease at a surface coverage below 100%, BslA should require less than 22 s to reduce the IFT of a droplet. At 0.03 mg.mL^{-1} the Regime I time for WT-BslA was 97 ± 18 s, compared to 12 ± 4 s for BslA-L77K, confirming that BslA-L77K adsorption is purely diffusion-limited, whereas WT-BslA faces an additional barrier to adsorption. As the protein concentration was increased or decreased, the corresponding Regime I times followed the power law predicted by Equation 1. We estimate the size of this energy barrier to be small, at ~5–9 k_BT (SI).

BslA undergoes a conformational change to a structure enriched in β-sheet upon binding to an oil-water interface. To study the conformation of BslA in aqueous solution and at an oil-water interface, circular dichroism (CD) spectroscopy of WT-BslA and the L77K mutant was performed in refractive index matched emulsions (RIMEs) (25). Refractive index matching enables the generation of oil-in-water emulsions without the light scattering that interferes with spectroscopic measurements. The folding of WT-BslA and BslA-L77K was very similar at pH 7 in phosphate buffer, with both curves exhibiting a maximum at ~205 nm, a minimum at ~212 nm and a shoulder at ~226 nm (Figure 3a). The minimum at ~212 nm is consistent with some β-sheet structure, whereas the minimum at <200 nm suggests a significant contribution from random coil. On binding to the interface of decane-water emulsions, the CD spectra of both WT-BslA and BslA-L77K are altered substantially (Figure 3b), exhibiting a positive signal below 200 nm and a minimum at 215 – 218 nm. Such features indicate a structural change to a form enriched in β-sheet (26).

WT-BslA forms a highly ordered 2D rectangular lattice at the air-water interface, whereas the BslA-L77K molecules are more disordered. Transmission electron microscopy (TEM) of WT-BslA stained with uranyl acetate indicates that the protein forms a highly ordered rectangular lattice (Figure 4a). Multiple domains of the WT-BslA lattice could be observed in any location on the grid. The observed domain areas varied from as small as 1000 nm^2 (~50 BslA molecules) up to 200000 nm^2 (>10000 BslA molecules). Less ordered "inter-domain" areas were also observed. Performing a Fast Fourier Transform (FFT) on TEM images of WT-BslA (Figure 4a, insets) revealed a rectangular lattice ($\alpha=\beta=90^o$, $a\neq b$) with dimensions of $d(10)$ = 3.9 nm and $d(01)$ = 4.3 nm. TEM images of BslA-L77K revealed a predominantly disorganised arrangement of protein, which nonetheless contained patches of rectangular packed protein (Figure 4b). The largest BslA-L77K domain size observed was approximately 20000 nm^2 (1250 BslA molecules). FFT on ordered domains of BslA-L77K revealed that the lattice parameters ($d(10)$ = 3.9 nm, $d(01)$ = 4.3 nm, $\alpha = \beta = 90^o$) were identical to the WT-BslA lattice (Figure 4b, insets).

The crystal structure of decameric BslA reveals two distinct structural forms. Although the crystal structure of WT-BslA features a large hydrophobic cap that allows the molecule to become anchored to a hydrophobic interface, kinetic measurements using the pendant drop method indicated that WT-BslA must overcome an energy barrier prior to or during adsorption (Figure 2). The fact that WT-BslA exhibits an adsorption barrier suggests that the hydrophobic residues in the cap region are not optimally oriented outwards in solution. Moreover, CD spectroscopy indicates a secondary structure change between the stable, monomeric form of the protein in aqueous solution, and the protein self-assembled at an interface. Analysis of the X-ray crystal structure (9) reveals two substantially different cap configurations in the decameric repeat unit. Eight of the ten subunits are positioned with their caps in close proximity to each other in a micelle-like arrangement. In these proteins, the cap regions are in a β-sheet configuration with the hydrophobic residues oriented outwards from the protein (Figure 5c), creating the oily core of the micelle. The remaining two subunits (chains I and J) are further away from the centre of the decamer (Figure 5a-b) and the cap regions are in a random coil configuration with many of the hydrophobic residues oriented inwards towards the protein (Figure 5d). This difference highlights the ability of the cap region to undergo substantial rearrangement in different solvent environments. The introduction of a positively charged amine would hinder this shielding mechanism as the lysine would orient outwards, forcing neighbouring hydrophobic residues to be exposed at the surface.

Mechanism of insertion and self-assembly of BslA at an interface. Coarse-grained molecular dynamics simulation of WT-BslA allowed us to estimate the energy required to remove the adsorbed protein from a model water-cyclohexane interface. The free energy of adsorption was reconstructed from pulling simulations by making use of the Jarzynski equality (27, 28) (see Supplementary Information for full description of methods). Our calculations show that the β-sheet cap configuration (chain C in the crystal structure) favourably increased the free energy of binding of BslA to the interface compared to the random coil cap configuration (chain I), despite the fact that the two forms are

chemically identical. Specifically, the calculated free energy of adsorption (ΔG) of chain C was 107.9 ± 0.7 k_BT, whereas the ΔG of chain I was just over half this value, at 59.3 ± 0.7 k_BT. Thus, the more structured form of the protein, even in the absence of intermolecular interactions, is more tightly adsorbed to the interface. The large difference in ΔG between WT-BslA chain C and chain I supports the hypothesis that chain C represents the conformation at an interface, while chain I represents the structure of BslA in solution. Moreover, the average orientation of the longest axis of the two forms of the protein at the interface was significantly different: chain C positioned itself at an angle of ~29.5º to the normal, whereas chain I was significantly more tilted at ~55.0º. We hypothesise that the less tilted conformation facilitates inter-protein interactions in the interfacial lattice.

Substituting the leucine at position 77 for lysine reduced ΔG for chain C to 85.2 ± 0.6 k_BT, although ΔG for L77K chain I (59.5 ± 0.6 k_BT) was similar to WT-BslA. Chains C and I of BslA-L77K were oriented at similar angles to WT chains. If we make the simplifying assumption that chain C represents the interfacial form of the protein and chain I the form in aqueous solution, and ignore energetic contributions arising from structural rearrangements, the $\Delta\Delta G$ associated with interfacial partitioning is 48.6 k_BT for the wild-type protein and 25.7 k_BT for the mutant, which may provide insight into the apparent ease with which the L77K mutant is removed from the interface following film compression. However, in order to make a direct comparison between the two proteins in our simulations, we directly replaced Leu-77 with lysine with no concomitant structural changes, whereas given that the introduction of the lysine eliminates the barrier to adsorption at the interface it is likely that the mutation causes significant rearrangement of the CAP1 strand and an increased exposure of neighbouring hydrophobic moieties.

Discussion

Details of the components that make up the biofilm matrix have been elucidated for several species of bacteria (1, 4). However information at the molecular and biophysical level regarding how these molecules contribute to biofilm stability, and how they assemble in the three dimensions of the bacterial community is largely lacking. Here we have illuminated the mechanism by which BslA, a protein made by all members of the *B. subtilis* biofilm community, selectively assembles at the interface of the biofilm. This mechanism is summarised in Figure 6 where a schematic for the adsorption of WT-BslA compared to BslA-L77K is depicted. In both cases, the monomeric protein adsorbs to the interface, although our data show that the rate of adsorption of BslA-L77K is greater as it experiences no barrier. After adsorption, both WT-BslA and BslA-L77K refold into structures enriched in β-sheet, but only WT-BslA can organise into an extensive, highly ordered 2D rectangular lattice. It is the high free energy of adsorption, combined with formation of a stable lattice structure that enhances the stability of WT-BslA interfacial films, so that introducing a small amount of compression is insufficient to remove WT-BslA from the interface (9). The apparently low elastic modulus of the resulting film (Fig 1) may also facilitate the irregular and highly wrinkled morphology of *B. subtilis* biofilms This is in contrast to BslA-L77K, which has a lower free energy of adsorption and does not form an organised lattice over the entire droplet surface and is thus easily removed from the interface by compression of the film..

At the interface BslA undergoes a structural metamorphosis. We infer this from CD data indicating that WT-BslA contains significant random coil content in solution, which is replaced by β-sheet after adsorption to an oil-water interface. Evidence from analysing the decameric crystal structure of BslA indicates that it is the hydrophobic cap of WT-BslA that undergoes the conformational transition (Fig 5). Thus, the mechanism of stabilisation of the hydrophobic patch in BslA is fundamentally different to that observed for the fungal hydrophobins: instead of the network of conserved disulphide bonds required to stabilise the energetically unfavourable surface exposure of hydrophobic amino acids observed in the hydrophobins, BslA has evolved structural plasticity in the three-stranded cap that allows conformational rearrangement at an interface. Once the molecule adsorbs to the interface the residues within the cap refold to reach a free energy minimum in which the hydrophobic residues protrude into the non-aqueous phase.

This structure-function relationship may be important for the function of BslA *in vivo*. As the BslA coding region is expressed throughout the entire *B. subtilis* biofilm population (8), the molecule needs to diffuse through the extracellular matrix to the surface of the biofilm without hindrance. A cap that becomes significantly more

hydrophobic after adsorption would be a useful mechanism to help to prevent unwanted interactions leading to retention of BslA within the body of the biofilm community. It should however be noted that this does not preclude other potential transport mechanisms to the biofilm interface such as the involvement of a chaperone protein. Moreover, these findings open up the possibility that the alternative conformational form of BslA has additional functions within the confines of the biofilm unrelated to its function in conferring hydrophobicity at the biofilm surface.

We performed all experiments on monomeric BslA, and moreover complementary experiments with dimeric BslA indicated that it is the monomeric unit that mediates the observed interfacial activity (Fig S3). Native BslA contains two cysteine residues towards the C-terminus in a 'CxC' motif, and we cannot rule out an additional stabilising contribution from disulphide formation at the elevated local protein concentrations present in the interfacial layer. This is unlikely to be the origin of the observed difference in stability of WT-BslA and L77K-BslA films under compression, however, since the cysteines are unchanged. Moreover, our simulations show that the wild-type and mutant proteins are inserted into the interface in similar orientations and with the same tilt angle, suggesting that there is unlikely to be any orientational barrier to disulphide bond formation by the mutant protein at the interface. One further possibility for the interfacial stability is that the three-stranded β-sheet cap mediates inter-protein interactions via formation of an extended intermolecular hydrogen-bonded β-sheet. This is likely to be disrupted in the L77K mutant if the CAP1 strand is sufficiently distorted by the preference of the introduced lysine residue for the aqueous environment.

The amphiliphilic nature of the fungal hydrophobins has led to suggestions for many potential applications, and these may be equally relevant to BslA. Hydrophobins have been proposed for use as surface modifiers and coating agents (29), and as emulsifiers, foam stabilisers and surfactants in many application areas including the food industry (30). The slow kinetics of adsorption will be an important factor to consider when attempting to use BslA in any applications, particularly where other surfactants are present. It has been shown, for example, that Class I hydrophobins adhere more strongly to interfaces than the Class II proteins, but that the Class II species can successfully compete to form a mixed interfacial membrane (31). Unlike BslA, however, Class II hydrophobins exhibit no barrier to interfacial adsorption, whereas the rapid adsorption of any competing species is likely to modulate BslA interfacial activity. Nonetheless, the structured self-assembly of BslA offers many opportunities for surface modification with nanoscale control.

Materials and Methods

Full details of all methods used are provided in *SI text*.

Protein purification. BslA was purified after expression as a GST fusion protein using standard techniques. See *SI text* for full details.

Circular dichroism (CD) spectropolarimetry. CD was performed using a Jasco J-810 spectropolarimeter. Control samples were analysed at a concentration of 0.1 $mg.mL^{-1}$ (6.7 μM) in a 0.1 cm quartz cuvette. Refractive index matched emulsions were analysed in a 0.01 cm demountable quartz cuvette. Measurements were performed with a scan rate of 50 $nm.sec^{-1}$, a data pitch of 0.1 nm and a digital integration time of 1 sec.

Pendant drop tensiometry. Monitoring the kinetics of BslA adsorption was achieved using pendant drop tensiometry with drop shape analysis. A Krüss Easydrop tensiometer (Krüss GmbH, Germany) was used in combination with Drop Shape Analysis software. See *SI text* for full details.

Transmission electron microscopy. BslA-WT and L77K samples were deposited onto carbon-coated copper grids (Cu-grid) (TAAB Laboratories Equipment Ltd) and imaged using a Philips / FEI CM120 BioTwin transmission electron microscope. See *SI text* for full details.

ACKNOWLEDGMENTS. We would like to thank the Edinburgh Protein Production (Biophysical Characterisation) Facility for use of circular dichroism spectroscopy and Dr. Colin Hammond for assistance with the SEC-MALLS experiment. This work was supported by EPSRC grant [EP/J007404/1] and BBSRC grants [BB/L006979/1; BB/I019464/1; BB/L006804/1]. Mass spectrometry analysis of purified proteins was performed in the College of Life Sciences and is supported by the Wellcome Trust [097945/B/11/Z].

REFERENCES

1. Flemming H-C, Wingender J (2010) The biofilm matrix. *Nat Rev Microbiol* 8:623–33.

2. Costerton JW, Lewandowski Z, Caldwell DE, Korber DR, Lappin-Scott HM (1995) Microbial biofilms. *Annu Rev Microbiol* 49:711 – 745.

3. Davey ME, O'Toole GA (2000) Microbial Biofilms : from Ecology to Molecular Genetics. *Microbiol Mol Biol Rev* 64:847–867.

4. Cairns LS, Hobley L, Stanley-Wall NR (2014) Biofilm formation by Bacillus subtilis: new insights into regulatory strategies and assembly mechanisms. *Mol Microbiol* 93:587–598.

5. Branda SS, Chu F, Kearns DB, Losick R, Kolter R (2006) A major protein component of the Bacillus subtilis biofilm matrix. *Mol Microbiol* 59:1229–38.

6. Kearns DB, Chu F, Branda SS, Kolter R, Losick R (2005) A master regulator for biofilm formation by Bacillus subtilis. *Mol Microbiol* 55:739–49.

7. Ostrowski A, Mehert A, Prescott A, Kiley TB, Stanley-Wall NR (2011) YuaB functions synergistically with the exopolysaccharide and TasA amyloid fibers to allow biofilm formation by Bacillus subtilis. *J Bacteriol* 193:4821–31.

8. Kobayashi K, Iwano M (2012) BslA(YuaB) forms a hydrophobic layer on the surface of Bacillus subtilis biofilms. *Mol Microbiol* 85:51–66.

9. Hobley L et al. (2013) BslA is a self-assembling bacterial hydrophobin that coats the Bacillus subtilis biofilm. *Proc Natl Acad Sci U S A* 110:13600–13605.

10. Linder MB, Szilvay GR, Nakari-Setälä T, Penttilä ME (2005) Hydrophobins: the protein-amphiphiles of filamentous fungi. *FEMS Microbiol Rev* 29:877–96.

11. Wösten HAB, De Vries OMH, Wessels JGH (1993) Interfacial Self-Assembly of a Fungal Hydrophobin into a Hydrophobic Rodlet Layer. *Plant Cell* 5:1567–1574.

12. De Vries OMH, Fekkes MP, Wösten HAB, Wessels JGH (1993) Insoluble hydrophobin complexes in the walls of Schizophyllum commune and other filamentous fungi. *Arch Microbiol* 159:330–335.

13. Hakanpää J et al. (2006) Two crystal structures of Trichoderma reesei hydrophobin HFBI — The structure of a protein amphiphile with and without detergent interaction. *Protein Sci* 15:2129–2140.

14. Torkkeli M, Serimaa R, Ikkala O, Linder M (2002) Aggregation and Self-Assembly of Hydrophobins from Trichoderma reesei: Low-Resolution Structural Models Thioflavin T staining. *Biophys J* 83:2240–2247.

15. Kobayashi K (2007) Gradual activation of the response regulator DegU controls serial expression of genes for flagellum formation and biofilm formation in Bacillus subtilis. *Mol Microbiol* 66:395–409.

16. Andreas JM, Hauser EA, Tucker WB (1938) Boundary Tension by Pendant Drops. *J Phys Chem* 42:1001–1019.

17. Stauffer CE (1965) The Measurement of Surface Tension by the Pendant Drop Technique. *J Phys Chem* 69:1933–1938.

18. Rosen MJ (2004) *Surfactants and Interfacial Phenomena* (J. Wiley & Sons, Hoboken, NJ). 3rd Ed.

19. Alexandrov NA et al. (2012) Interfacial layers from the protein HFBII hydrophobin: dynamic surface tension, dilatational elasticity and relaxation times. *J Colloid Interface Sci* 376:296–306.

20. Szilvay GR et al. (2007) Self-assembled hydrophobin protein films at the air-water interface: structural analysis and molecular engineering. *Biochemistry* 46:2345–54.

21. Jang H-S et al. (2014) Tyrosine-mediated two-dimensional peptide assembly and its role as a bio-inspired catalytic scaffold. *Nat Commun* 5:3665.

22. Tripp BC, Magda JJ, Andrade JD (1995) Adsorption of globular protein at air/water interface as measured by dynamic surface tension: Concentration dependence, mass-transfer considerations, and adsorption kinetics. *J Colloid Interface Sci* 173:16–27.

23. Beverung CJ, Radke CJ, Blanch HW (1999) Protein adsorption at the oil/water interface: characterization of adsorption kinetics by dynamic interfacial tension measurements. *Biophys Chem* 81:59–80.

24. Ward AFH, Tordai L (1946) Time-Dependence of Boundary Tensions of Solutions I. The Role of Diffusion in Time-Effects. *J Chem Phys* 14:453.

25. Husband FA, Garrood MJ, Mackie AR, Burnett GR, Wilde PJ (2001) Adsorbed Protein Secondary and Tertiary Structures by Circular Dichroism and Infrared Spectroscopy with Refractive Index Matched Emulsions. *J Agric Food Chem* 49:859–866.

26. Towell III JF, Manning MC (1994) in *Analytical Applications of Circular Dichroism*, eds Purdie N, Brittain HG (Elsevier, New York), pp 175–205.

27. Jarzynski C (1997) Nonequilibrium equality for free energy differences. *Phys Rev Lett* 78:2690–2693.

28. Park S, Schulten K (2004) Calculating potentials of mean force from steered molecular dynamics simulations. *J Chem Phys* 120:5946–5961.

29. Valo HK et al. (2010) Multifunctional Hydrophobin: Toward Functional Coatings for Drug Nanoparticles. *ACS Nano* 4:1750–1758.

30. Hektor HJ, Scholtmeijer K (2005) Hydrophobins: proteins with potential. *Curr Opin Biotechnol* 16:434–439.

31. Askolin S et al. (2006) Interaction and comparison of a class I hydrophobin from Schizophyllum commune and class II hydrophobins from Trichoderma reesei. *Biomacromolecules* 7:1295–1301.

32. Humphrey W, Dalke A, Schulten K (1996) VMD: visual molecular dynamics. *J Mol Graph* 14:33–38.

Figure Legends

Figure 1: (a) Interfacial tension profiles of a droplet of unfractionated WT-BslA (0.02mg.mL^{-1}) in air (black line) and in glyceryl trioctanoate (grey line). (b) A 50 µL droplet of WT-BslA (0.03 mg.mL^{-1}) on HOPG after 0 (left) and 30

(right) minutes. (c) A 25 μL droplet of WT-BslA (0.02 $mg.mL^{-1}$) in air before and after compression, (d) A 40 μL droplet of WT-BslA (0.2 $mg.mL^{-1}$) in glyceryl trioctanoate before and after compression

Figure 2: A plot of Regime I times versus concentration of WT-BslA (closed circles) and BslA-L77K (open circles). The dashed line represents the predicted time to reach a surface coverage of 1.57 $mg.m^{-2}$ using Equation 1.

Figure 3: (a) CD spectra of WT-BslA (black line) and BslA-L77K (grey line) in 25 mM phosphate buffer (pH 7). (b) CD spectra of refractive index matched emulsions stabilised by WT-BslA (black line) and BslA-L77K (grey line). Dotted lines: raw data; solid lines: smoothed [see SI].

Figure 4: TEM images of (a) WT-BslA and (b) BslA-L77K stained with uranyl acetate. Scale bar = (a) 100 nm and (b) 50 nm. Insets: FFTs of (i) The entire TEM image, (ii) the selected square area in each image. The numbers in (a)(ii) correspond to the Miller indices of the 2D lattice structure.

Figure 5: (a) The BslA decamer from PDB file 4BHU (9) with chains A-H displayed in cyan and chains I and J in red. The hydrophobic caps are displayed as surface representations, while the rest of the chains are displayed as cartoon backbone representations. (b) A depiction of the hydrophobic core of the decamer with the hydrophobic caps of chains A-H in cyan and the hydrophobic caps of chains I and J in red. (c) A depiction of chain C, showing the hydrophobic residues (black) oriented outwards as opposed to (d) chain I, in which the hydrophobic residues have no particular orientation. Images generated using Visual Molecular Dynamics (32).

Figure 6: Schematic of BslA adsorption. When unbound, the conformation of the hydrophobic cap of WT-BslA orients the hydrophobic residues away from the aqueous medium, slowing the rate of adsorption (indicated by a small arrow). The L77K mutation removes the adsorption barrier by exposing some or all of the hydrophobic residues within the hydrophobic cap, increasing the rate of adsorption (indicated by a bold arrow). Once adsorbed onto the interface, the surface-bound WT-BslA refolds to a conformation rich in β-sheet and is able to form strong lateral interactions with adjacent molecules, forming an organised lattice that under normal circumstances will not be removed from the interface (indicated by the crossed arrow). Surface bound BslA-L77K forms a less well-organised lattice and can be removed from the interface with only minimal energy, such as droplet compression.

Figure 1

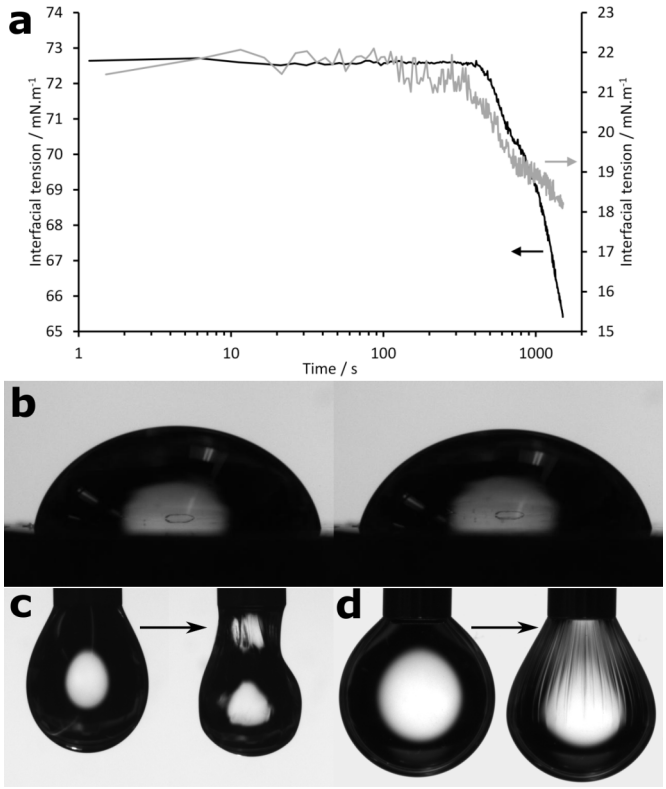
a
Interfacial tension / mN.m-1
Interfacial tension / mN.m-1
Time / s
b
c
d

Figure 2

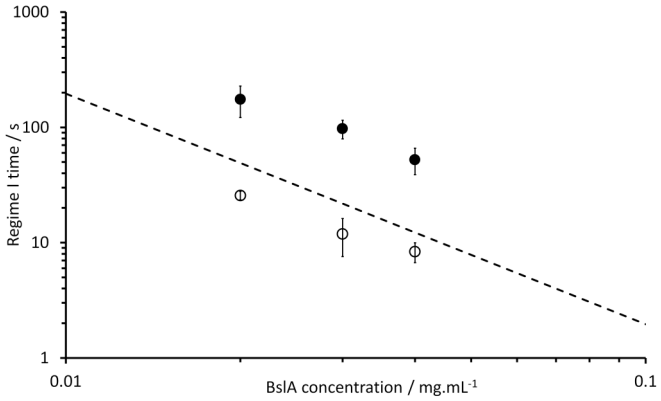

Figure 3

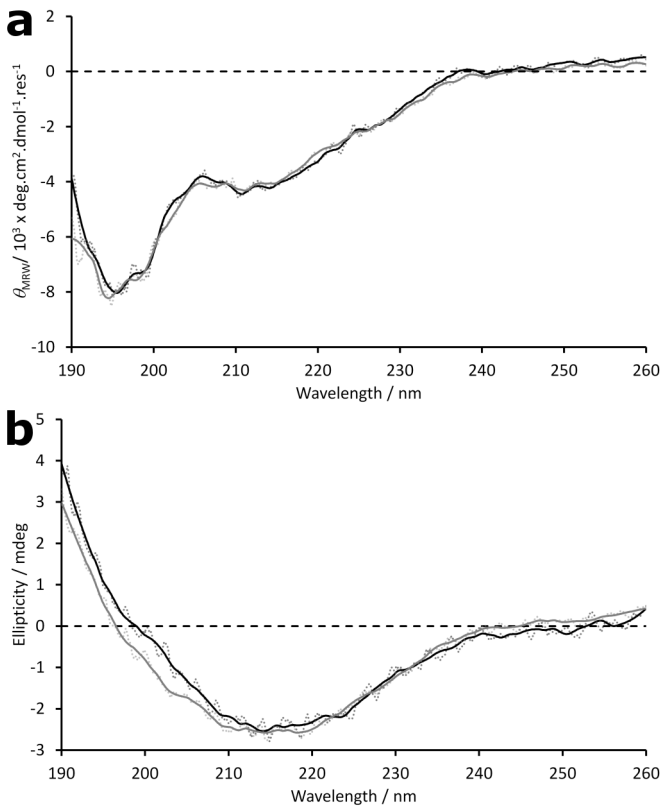
a
2
0
-2
-4
-6
-8
-10
θ_{MRW}/ 10^3 x deg.cm^2.dmol^{-1}.res^{-1}
190
200
210
220
230
240
250
260
Wavelength / nm
b
5
4
3
2
1
0
-1
-2
-3
Ellipticity / mdeg
190
200
210
220
230
240
250
260
Wavelength / nm

Figure 4

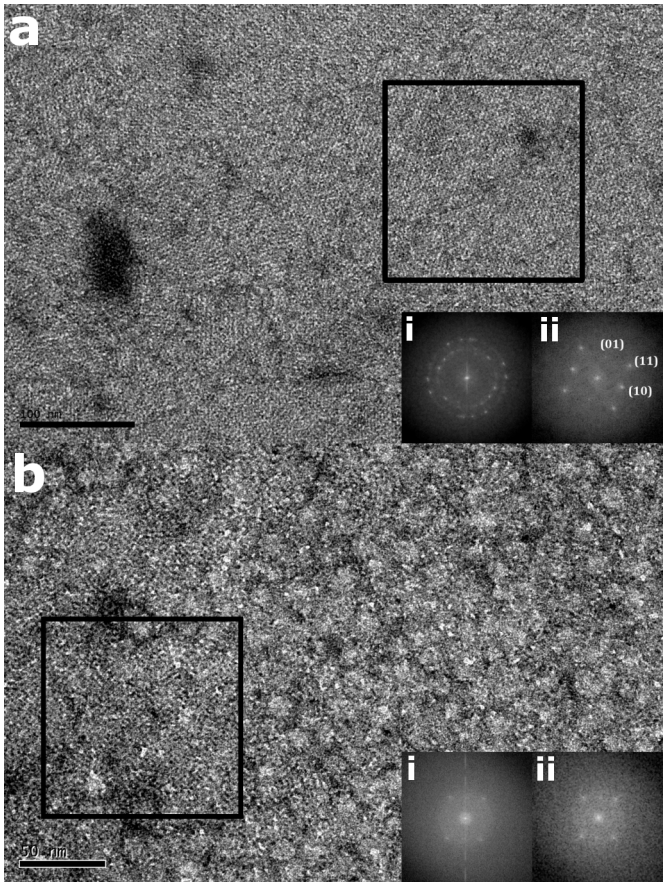

Figure 5

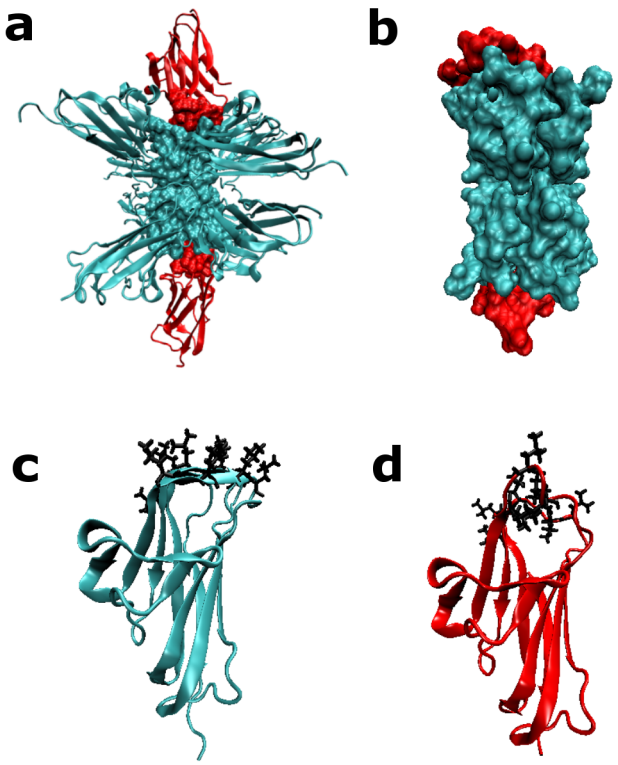

Figure 6